Plastic mechanism analysis of CHS stub columns strengthened using CFRP

M. Elchalakani
School of Architectural, Civil and Mechanical Engineering, Victoria University, Melbourne, Australia

M.R. Bambach
Department of Civil Engineering, Monash University, Melbourne, Australia

ABSTRACT: This paper presents a plastic mechanism analysis for circular hollow section (CHS) tubes strengthened using carbon fiber reinforced polymer (CFRP) deforming in an axi-symmetric (elephant foot) collapse mode under large deformation axial loading. The collapse proceeded progressively by folding about three concentrated hinge lines and hoop extension of the shell. An expression for the plastic collapse axial load was obtained by equating the total energy absorbed in bending and extension to the external work carried out during deformation of the tube. The newly derived mathematical model takes into account the contribution of the CFRP towards energy absorption during collapse. Comparisons of the predicted instantaneous post-buckling collapse loads with those obtained from experiments carried out elsewhere show good agreement.

1 INTRODUCTION

Hollow steel tubes are widely used as columns in many structural systems and a common failure mode of such tubes when subjected to axial compression (or combined loading) is local buckling near a column end. For example hollow steel tubes are used as bridge biers in Japan and such piers suffered exten- sive damage and even collapse during the 1995 Hyogoken-nanbu earthquake [1]. One of the meth- ods used to in seismic retrofit of such bridge piers is the use of CFRP rapping (see Fig 1). Thus, it is im- portant to predict the response of the composite sec- tion (CHS+CFRP) under large deformation axial compression. Plastic mechanism analysis is widely used to derive such predictions.

(a) Typical Column

(b) Anti-symmetric mode of collapse

(c) Elephant foot with a fracture

Figure 1.   Damaged bridge piers in Japan [1].

The collapse mechanisms of tubular stub columns were studied in the past by Johnson et al [2], Abramowicz and Jones [3], and Meng et al [4]. Wierzbicki Abramowicz [5] used velocity filed approach to derive general formulations for the crushing of thin-walled structures. The basic folding of an isolated plate forming the roof mechanism was studied by Davies et al [6] and Mahendran [7]. Ohkubo et al [8] provided an expression for the mean crushing load of hat sections commonly used in the Automotive industry where they showed that the radius of the rolling hinge has significant effect on such load. Mamalis et al [9] studied non-metallic plastic square tubes under axial load. The effect of CFRP on the collapse of composite circular tubes was studied by Mamalis et al [10], Song et al [11], Gupta and Abbas [12], Hanefi and Wierzbicki [13] and more recently by Wang and Lu [14]. However, these precious crush studies derive formulations for the mean crush load and little research focused on the development of the collapse curves such as Key and Hancock [15], Zhao et al [16], Grzebieta [17] and more recently Elchalakani et al [18, 19] for bending of CHS.

Grzebieta [17] developed formulation for the instantaneous axial collapse load versus axial deflection for an empty CHS forming an axi-symmetric collapse mode. It is shown in this paper that his rigid plastic mechanism is modified to include the effects of the finite length of the plastic hinges and the CFRP strengthening. The newly derived collapse curves and those developed by Grzebieta's [17] will be compared against experimental collapse curves obtained recently by Teng and Hu [1].

2 PREDICTION OF COLLPASE CURVES

2.1 *Effect of CFRP*

Consider the bimetallic plate (shown in Fig. 2) consisting of fully adhering different materials of thickness ts (for CHS flats) and t_f for (FRP sheet) and corresponding yield stresses σ_{ys} and σ_{yf}, respectively. Examining the full yielding of the composite cross section of overall thickness $t = t_s + t_f$ and unit width and requiring the forces on the composite section we obtain the position of the plastic neutral axis x from
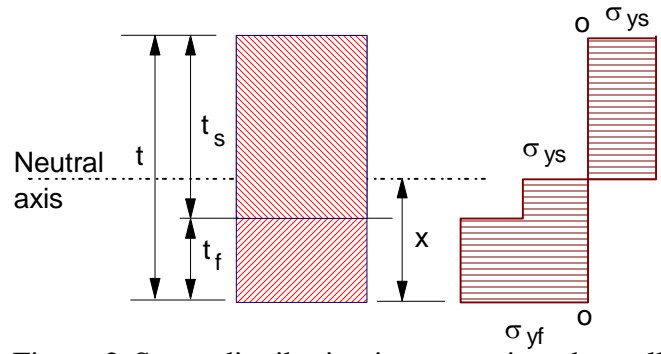

Figure 2. Stress distribution in composite tube wall.

$$\sigma_{ys}(t-x) = \sigma_{ys}(x-t_f) + \sigma_{yf}t_f \qquad (1)$$

$$x = \frac{\sigma_{ys}(t+t_f) - \sigma_{ys}t_s}{2\sigma_{ys}} \qquad (2)$$

To evaluate the full plastic moment per unit width to bend plastically the composite section M_p we take moment about the neutral axis

$$M_p = \sigma_{ys}\frac{(t-x)^2}{2} + \sigma_{ys}\frac{(x-t_f)^2}{2} + \sigma_{yf}t_f(x-\frac{t_f}{2}) \qquad (3)$$

Introducing the dimensionless ratios $k_f = \sigma_{yf}/\sigma_{ys}$ and $t_r = t_f/t_s$, Equation 3 can be written as

$$M_p = (1 + 2kt_r + 2kt_r^2 - k^2t_r^2)\frac{\sigma_{ys}t_s^2}{4} \qquad (4)$$

Expressing the full plastic moment M_p in a relation to equivalent yield stress for the face (σ_{yf}')

$$\sigma_{yf}' = \frac{1 + 2k_f t_r + 2k_f t_r^2 - k_f^2 t_r^2}{(1+t_r^2)}.\sigma_{ys} \qquad (5)$$

2.2 *Work dissipated by bending*

The key mechanical properties of the mild steel specimens reinforced using normal modulus CRP sheets tested in [1] are listed in Table 1. The geometry of the CHS and the external CFRP sheets are shown in Figure 3. The elastic modulus of the steel and CFRP sheet was 201 and 80.1 GPa, respectively. The stub columns were about 500 mm long and tested under uniform axial compression. The theoretical expressions for the energy components consumed in bending and hoop stretching are developed below and combined to give the overall load-axial displacement relationship for the composite section.

Table 1.   Details of specimens [1].

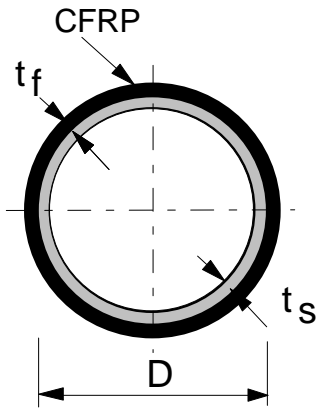| Spec.	D mm	t_s mm	σ_{ys} MPa	σ_{yf} MPa	t_f mm	t_r (=t_f/t_s)
ST-F0	165	4.2	333	0.00	0.0	0.000
ST-F1	166	4.2	333	1825	0.17	0.040
ST-F2	165	4.2	333	1825	0.34	0.081
ST-F3	166	4.2	333	1825	0.51	0.121

Figure 3. Geometry of SHS+CFRP.

Figures 4 and 5 show the outward folding mechanism and its kinematics, respectively, developed at large axial deformations. The deformation energy consumed during bending at the three plastic hinges in Fig 5 (A, $\overline{AB}$ and B) of the outward folding mechanism can be expressed as

$$dW_b = 4\pi(R_A + R_B)M_p d\alpha \tag{6}$$

in which α is the angular change defined in Figure 5, R_A and R_B are the radii of the deformed tube at the plastic hinges A and B, and $M_p = \sigma'_{yf} t^2/4$. Note that $R_A = R$ and $\rho_\alpha = L/2$ and

$$R_B = R + 2\rho_\alpha(1 - \cos\alpha) = R + \frac{L(1 - \cos\alpha)}{\alpha} \tag{7}$$

Using Equation 7, Equation 6 can be simplified to

$$dW_b = 4\pi M_p\left(2R + \frac{L(1 - \cos\alpha)}{\alpha}\right)d\alpha \tag{8}$$

where α is the angular change at the plastic hinge A or B in Figure 5. L is the half-wave length of the elephant foot mechanism which was assumed constant during the course of deformation.

2.3 *Work dissipated by hoop extension*

As the tube is compressed, the tube expands in the hoop direction. The deformation energy for the elephant foot due to this expansion can be given by

$$dW_h = \pi\sigma_\theta tL^2 \cos\zeta d\zeta \tag{9}$$

Knowing that $\zeta = \alpha/2$ and assuming full composite action in the hoop direction using Equation 5, ie, $\sigma_\theta = \sigma'_{yf}$, where σ_θ is the hoop stresses, γ is an angle defined in Figure 5 and ρ_α is the current radius. Thus Equation 9 can be simplified from the kinematical relations given in Figure 5 to
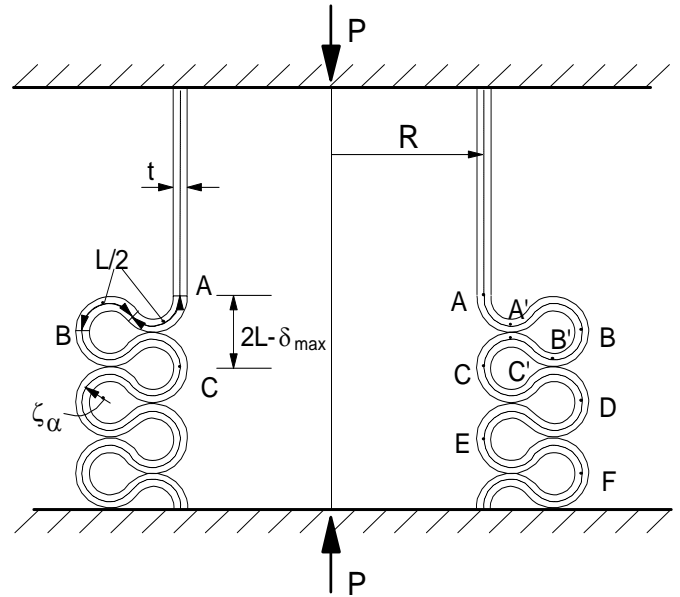

Figure 4. The theoretical model.

$$dW_h = \frac{4\pi\sigma'_{yf} tL^2 \sin^2(\alpha/2)\cos(\alpha/2)}{\alpha^2}d\alpha \tag{10}$$

Most of the work carried out by the internal forces have now been determined and can be summed and equated to the work carried out by those forces external to the structure ($dW_{ext} = dW_{int}$). This external energy can be expressed as

$$dW_{ext} = P \cdot d\delta \tag{11}$$

$$\delta = 2L(1 - \frac{\sin\alpha}{\alpha}) \tag{12}$$

$$dW_{ext} = P.d\delta = 2PL\left(\frac{\sin\alpha - \alpha\cos\alpha}{\alpha^2}\right)d\alpha \tag{13}$$

where δ is the axial displacement and α is the total angular change shown in Figure 5. Therefore, denoting the increment of rotation $d\alpha$, the instantaneous post buckling collapse load can be written as

$$P = \frac{4\pi M_p\left(2R + \frac{L(1 - \cos\alpha)}{\alpha}\right)\alpha^2}{2L(\sin\alpha - \alpha\cos\alpha)} +$$

$$\frac{4\pi\sigma'_{yf} tL^2 \sin^2(\alpha/2)\cos(\alpha/2)}{2L(\sin\alpha - \alpha\cos\alpha)}$$
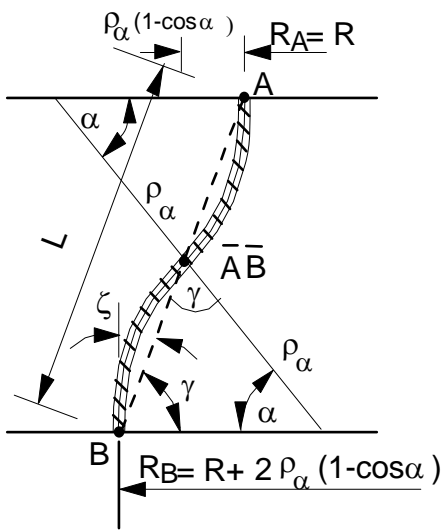
$$\tag{14}$$

Figure 5. Mechanism kinematics.

Note, the contribution of the CFRP is depicted in the 1st and 2nd terms in Equation 14 which represents the energy consumed in the bending and hoop extension, respectively. Note, in the tests the CFRP sheets were rapped in the hoop direction, where it has no strength in the axial direction. The collapse curves can be plotted by first assuming a value for α and substituting in Equation 14, the value of P can be readily determined. From the geometrical compatibility given in Equation 12, δ can be computed.

A similar Equation can be derived by slightly modifying Equation 23 in Reference [17] by assuming full composite action in the hoop direction as follows

$$P = \left\{ \frac{2t\sigma'_{yf}\left(2R + \dfrac{L(1-\cos\alpha)}{\alpha}\right)}{\sqrt{3}} + \frac{4\sigma'_{ys}L^2\sin^2(\alpha/2)\cos(\alpha/2)}{\alpha^2} \right\} \frac{\pi t t L^2 \alpha^2}{2L(\sin\alpha - \alpha\cos\alpha)}$$

(15)

Note $L = 1.347\sqrt{Rt}$ was adopted in Grzebieta [17] and subsequently was used in Equation 15. A slightly larger average value of $L = 1.843\sqrt{Rt}$ was used in Equation 14. A larger half-wave length was used in the numerical modelling performed by Teng and Hu [1] to match the experimental collapse curves for the plain and strengthened CHS specimens.
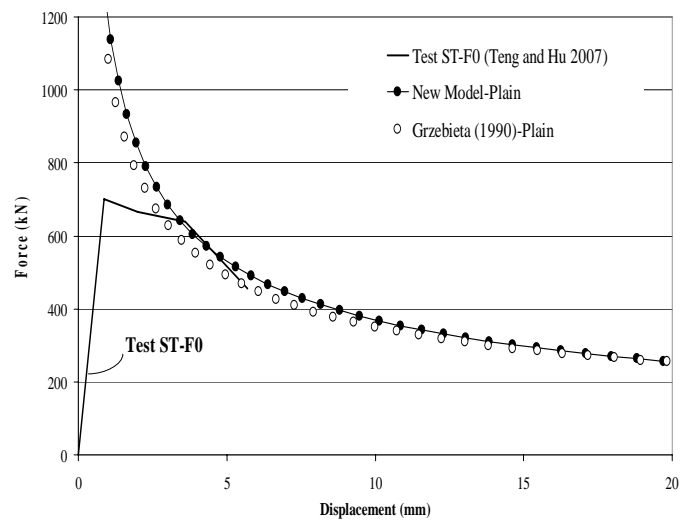

Figure 6. Analysis results for ST-F0[*]

3 RESULTS OF THE ANALYSIS

The collapse curves predicted using both Equations 14 (the New Theory) and 15 (Grzebieta [17]) are plotted in Figures 6 to 9 together with the experimental curves for all the specimens tested recently by Teng and Hu [1]. Test specimen ST-F0 represents a plain CHS with no strengthening. Specimens ST-F1, ST-F2 and ST-F3 represent CHS strengthened with one, two and three layers of CFRP sheets, respectively. It is seen that there is a good agreement in the slope of the collapse curve and values of the post-buckling axial load particularly at large axial deformations. It is also seen that Grzebieta [17] model for plain CHS significantly underestimates the axial load, but its modified version (Equation 15) provides reasonable predictions. It is seen that Equation 15 under estimates the axial load compared to Equation 14. It appears that adding more layers after

---

[*] Refer Appendix for Figure 7-9

strengthening with 2 layers of CFRP does not have significant effect on strength. This is also shown correct by the new model.

4 CONCLUSIONS

This paper presented a plastic mechanism analysis for circular hollow section (CHS) tubes strengthened using carbon fibre reinforced polymer (CFRP) deforming in an axi-symmetric (elephant foot) collapse mode under large deformation axial loading. The collapse proceeded progressively by folding about three concentrated hinge lines and hoop extension of the shell. An expression for the plastic collapse axial load was obtained by equating the total energy absorbed in bending and extension to the external work carried out during deformation of the tube. The newly derived mathematical model takes into account the contribution of the CFRP towards energy absorption during collapse. Comparisons of the predicted instantaneous post-buckling with those obtained from experiments carried out elsewhere show good agreement.

REFERENCES

1. Teng, J.G. and Y.M. Hu, *Behaviour of FRP-Jacketed Circular Steel Tubes and Cylindrical Shells under Axial Compression.* Construction and Building Materials, 2007. 21(9): p. 827-838.

2. Johnson, W., Soden, P. D. and S.T.S. Al-Hassani, *Inextensional Collapse of Thin-Walled Tubes under Axial Compression.* Journal of Strain Analysis, 1977. 12(4): p. 317-330.

3. Abramowicz, W. and N. Jones, *Dynamic Progressive Buckling of Circular and Square Tubes.* International Journal of Impact Engineering, 1984a. 4(4): p. 243-270.

4. Meng, Q., Al-Hassani, S. T. S. and P.D. Soden, *Axial Crushing of Square Tubes.* International Journal of Mechanical Science, 1983. 25(9-10): p. 747-773.

5. Wierzbicki, T. and W. Abramowicz, *On the Crushing Mechanics of Thin-Walled Structures.* Journal of Applied Mechanics, 1983c. 50: p. 727-734.

6. Davies, P., Kemp, K. O. and A.C. Walker, *An Analysis of the Failure Mechanism of an Axially Loaded Simply Supported Steel Plate.* Proceedings of Institute of Civil Engineers, 1975. 25(Part 2): p. 645-658.

7. Mahendran, M., *Local plastic mechanisms in thin steel plates under in-plane compression.* Thin-Walled Structures, 1997. 27(3): p. 245-261.

8. Ohkubo, Y., Akamatus, T. and K. Shirasawa, *Mean Crushing Strength of Closed-Hat Section Members.* Society of Automotive Engineers, 1974. Paper 740040: p. 1-12.

9. Mamalis, A.G., Manolakas, D.E., Baldoukas, A.K. and G.L. Viegelahn, *The Axial Crushing of Thin Walled Steel PVC Tubes and Frusta of square Cross Section.* International Journal of impact Engineering, 1989b. 8(3): p. 241-264.

10. Mamalis, A.G., Manolakas, D.E., Demosthenous, G.A. and Johnson, W., *Axial Plastic Collapse of Thin Bi-Material Tubes as Energy Dissipating Systems.* International Journal of impact Engineering, 1991. 11(2): p. 185-196.

11. Song, H.-W., et al., *Axial Impact Behaviour and Energy Absorption Efficiency of Composite Wrapped Metal Tubes.* International Journal of impact Engineering, 2000. 24(2): p. 385-401.

12. Gupta, N.K. and H. Abbas, *Lateral Collapse of Composite Cylindrical Tubes between Flat Platens.* International Journal of impact Engineering, 2000. 24(2): p. 329-346.

13. Hanefi, E.H. and T. Wierzbicki, *Axial Resistance and Energy Absorption of Externally Reinforced Metal Tubes.* Composites, Part B, 1996. 27B: p. 387-394.

14. Wang, X. and G. Lu, *Axial Crushing Force of Externally Fibre-Reinforced Metal Tubes.* Proceedings of the Institute of Mechanical Engineers, 2002. 216(863-873).

15. Key, P.W. and G.J. Hancock. *Plastic Collapse Mechanisms for Thin-Walled Cold Formed Square Tube Columns.* in *10th Australian Conference on the Mechanics of Structures and Materials.* 1986. The University of Adelaide.

16. Zhao, X.-L., B. Han, and R.H. Grzebieta, *Plastic mechanism analysis of concrete-filled double-skin (SHS inner and SHS outer) stub*

eJSE
International

columns. Thin-Walled Structures, 2002. 40(10): p. 815-833.

17. Grzebieta, H., *An alternative Method for Determining the Behaviour of Round Stocky Tubes subjected to an Axial Crush Load.* Thin-Walled Structures, 1990. 9: p. 61-89.

18. Elchalakani, M., X.L. Zhao, and R.H. Grzebieta, *Plastic mechanism analysis of circular tubes under pure bending.* International Journal of Mechanical Sciences, 2002. 44(6): p. 1117-1143.

19. Elchalakani, M., Zhao, X. L., Grzebieta, H., *Plastic Collapse Analysis of Slender Circular tubes Subjected to Large Deformation Pure Bending.* Advances in Structural Engineering -An International Journal 2002a. 5(4): p. 241-257.
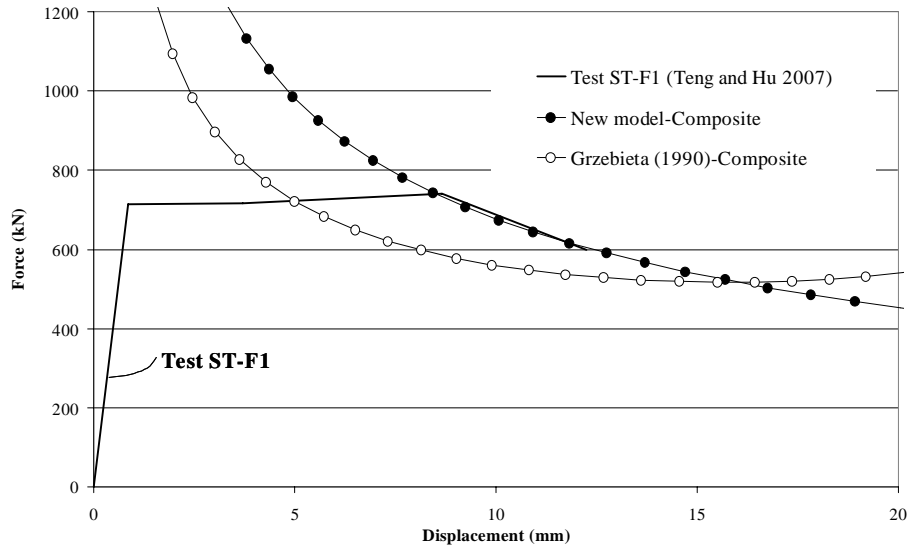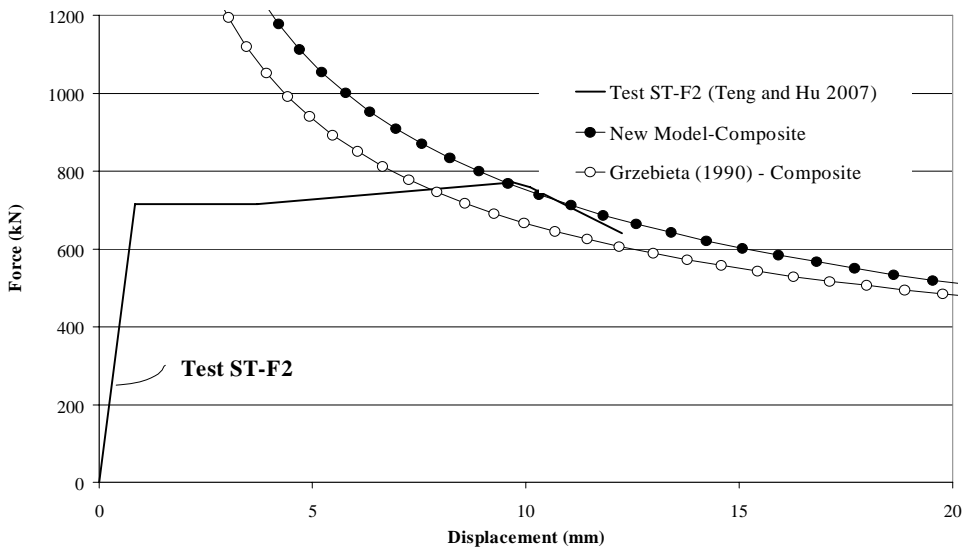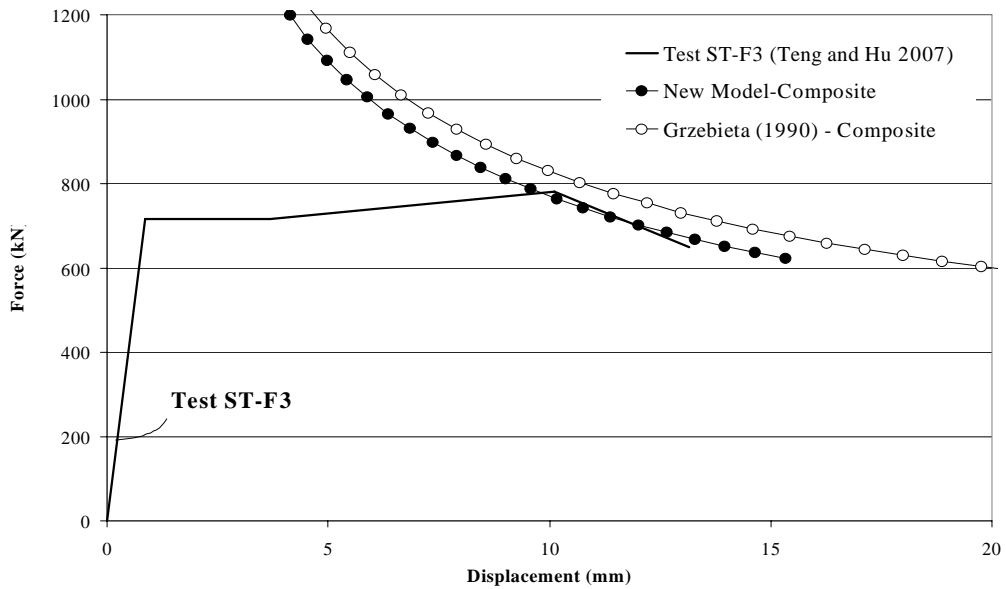
Appendix

Figure 7 Analysis results for ST-F1

Figure 8 Analysis results for ST-F2

Figure 9 Analysis results for ST-F3